

Effect of Hydrogen-Rich Water on Gut Microbiota in Mice With High-Fat Diet

Guijiao Xie

First Affiliated Hospital of Nanchang University

Zelin Liu

the fourth attached hospital of nanchang university

Jiao Wang

First Affiliated Hospital of Nanchang University

Shasha He

First Affiliated Hospital of Nanchang University

Honghong Liu

First Affiliated Hospital of Nanchang University

Jixiong Xu (✉ Jixiong.Xu@ncu.edu.cn)

First Affiliated Hospital of Nanchang University

Research Article

Keywords: Hydrogen-rich water, Oxidative stress, Gut microbiota, High-fat diet

DOI: <https://doi.org/10.21203/rs.3.rs-606685/v1>

License:   This work is licensed under a Creative Commons Attribution 4.0 International License.

[Read Full License](#)

1 **Effect of hydrogen-rich water on gut microbiota in mice with high-fat diet**

2 Guijiao Xie ¹; Zelin Liu²; Jiao Wang ¹; Shasha He¹; Honghong Liu¹; Jixiong Xu^{1*}

3 ¹ Department of Endocrinology and Metabolism, First Affiliated Hospital of
4 Nanchang University, Nanchang, P.R. China

5 ² Department of Endocrinology and Metabolism, Fourth Affiliated Hospital of
6 Nanchang University, Nanchang, P.R. China

7 * **Corresponding Author:** Jixiong Xu. Department of Endocrinology and
8 Metabolism, First Affiliated Hospital of Nanchang University, No.17 Yongwaizheng
9 St., Nanchang, Jiangxi Province, 330006 P.R. China. E-mail address:
10 Jixiong.Xu@ncu.edu.cn

11 Guijiao Xie and Zelin Liu contributed equally to this work.

1 **Abstract**

2 **Objective:** To investigate the effects of hydrogen-rich water (HGRW) on the structure
3 and composition of intestinal microflora in mice fed high-fat diets (HFDs).

4 **Materials and Methods:** C57BL/6 mice were divided into four groups: (1) normal
5 diet (CD)-normal water (W); (2) CD-HGRW; (3) HFD-W; and (4) HFD-HGRW.
6 After 12 weeks, we sampled fasting blood glucose, lipids, transaminases, and tissue
7 oxidative stress levels and measured body weight. High-throughput sequencing
8 technology was used to sequence the intestinal microflora and differences in intestinal
9 microflora were compared by group, using bioinformatics analysis.

10 **Results:** Body weight, oral glucose tolerance, and blood glucose increased
11 significantly in the HFD group compared with the CD group ($P < 0.001$), and
12 malondialdehyde levels were significantly increased in the livers of mice fed a HFD
13 ($P < 0.05$). Steatosis was seen in the liver parenchyma of the HFD group, and to a
14 lesser degree in the HGRW group. The richness and diversity of intestinal flora only
15 decreased significantly in the HFD group ($P < 0.05$). However, 24 genera and 26
16 species were significantly different between the HFD and CD subgroups of mice fed
17 HGRW. Nine genera and five species were significantly different between the HGRW
18 and W subgroups of mice fed a HFD. Correlations were confirmed for 10
19 physiological parameters; and were positively correlated with 17 genera in the HFD
20 group; six genera were negatively correlated in the HGRW group. Importantly,
21 *Lactobacillus* was closely related to tissue malondialdehyde levels.

22 **Conclusion.** Oral HGRW has beneficial effects against antioxidant stress and liver
23 damage. It may improve the diversity and structure of the intestinal flora, enhancing
24 the relative abundance of beneficial flora.

25 **Key words:** Hydrogen-rich water; Oxidative stress; Gut microbiota; High-fat diet

1 **Introduction**

2 The impact on human health of the intestinal flora, as a so-called microbial organ, has
3 gained increased research interest over the recent years. The human intestinal tract has
4 a complex micro-ecosystem of many microorganisms, mainly bacteria, with the total
5 number of intestinal microflora cells outnumbering human cells by a factor of 10 (this
6 increases to a 100-fold difference in the number of genes) [1,2]. These cells exist in a
7 symbiotic relationship, with the intestinal microflora having irreplaceable roles in
8 immune system activation, digestion, and nutrient absorption, resisting the invasion of
9 foreign pathogenic bacteria, and producing important metabolites and bioactive
10 substances [3,4].

11 The diversity of intestinal flora is particularly relevant to immune system
12 development in related humans. Studies in germ-free mice have shown that these
13 animals have reduced immunity and slow development, with insufficient intestinal
14 mucosal immunity and significant reductions in mesenteric lymph nodes and the
15 number of IgA-secreting plasma cells. Furthermore, the ability to fight against
16 pathogenic bacteria is significantly weakened[5]. However, after transplanting the
17 intestinal flora from ordinary mice, such manifestations can be reversed[6]. In fact,
18 the composition of intestinal microbes depends on host genetics, immunity, dietary
19 habits, intestinal PH, antibiotic use, and the impact of the disease [2]. Research into
20 the role of disease has shown that the occurrence and development of certain
21 metabolic, autoimmune, and other disorders is often closely related to a disordered
22 intestinal flora. Studies have shown that changes in the intestinal flora can affect lipid
23 metabolism, trigger low-level chronic systemic inflammation, and induce obesity and
24 insulin resistance [7,8]. Obesity, caused by abnormal or excessive fat accumulation
25 and increases in the risk of many chronic diseases, has been linked to changes in the
26 composition and function of intestinal flora in animal models [9]. Oxidative stress and
27 chronic low-grade inflammatory response are key promoters of obesity and its
28 associated complications [10,11].

29 Free radicals are necessary to life, forming the basis of energy metabolism and
30 often serving as important signaling molecules in cells. Under normal physiological

1 conditions, the production and scavenging of free radicals is a dynamic and balanced
2 process. However, when there are an abnormally high number of free radicals, the
3 resulting oxidative stress can damage body cells, DNA, lipids, and proteins [12,13].
4 Molecular hydrogen is an antioxidant that can rapidly diffuse to react with cytotoxic
5 reactive oxygen species to reduce oxidative stress [14]. Drinking hydrogen-rich water
6 (HGRW) increases the concentration of hydrogen molecules in blood and tissues. It
7 has been shown that drinking HGRW can inhibit weight gain in obese rats and
8 activate the expression of antioxidant defense genes [15].The human microbiome
9 project indicates that 70% of gastrointestinal microbial species have a genetic ability
10 to encode hydrogen metabolism, suggesting an important role for this element.
11 Studies have shown that the relative abundance of intestinal flora in mice that drink
12 molecular hydrogen-dissolved alkaline electrolyzed water is significantly different to
13 that in control mice, having a beneficial effect on cholesterol metabolism and
14 protecting against liver damage [16].

15 It is essential that we understand how HGRW can prevent intestinal
16 microecological imbalance in the context of a high-fat diet (HFD) and whether this
17 can promote the restoration of microecological balance to protect human health and
18 prevent related diseases. This study aimed to investigate the effect of HGRW on
19 intestinal flora and antioxidant stress in mice fed with HFD.

20 **Materials and methods**

21 *Preparation of HGRW*

22 We put 400 ml of double-distilled normal water (W) in a hydrogen-producing water
23 bottle (Yishui Technology co. LTD, Hangzhou, China).The bottle cap was tightened,
24 turned upside down, pressed and held the button for 5 min, and completed single
25 electrolysis hydrogen production to a saturation of 1200 parts per billion. HGRW was
26 freshly prepared before each relevant experiment to ensure high concentrations of
27 hydrogen. During the experiments, mice were given HGRW twice a day and gavage
28 was limited to between 09:00 and 15:00 h. Normal water was provided at the rest of
29 the time. These conditions were maintained for 12 weeks.

1 ***Animals and experimental design***

2 Male 6-week-old C57BL/6 mice weighing 20–25 g were obtained (Changsha Slake
3 Jingda Experimental Animal Co. Ltd., Hunan, China). All experimental procedures
4 were conducted in conformity with institutional guidelines for Medical Research
5 Ethics Committee of The First Affiliated Hospital of Nanchang University, and
6 conformed to the National Institutes of Health Guide for Care and Use of Laboratory
7 Animals. This experiment was approved by the ethics committee of the First Affiliated
8 Hospital of Nanchang University. During the experiment, mice were raised in
9 independent ventilated cages, with the number of mice per cage determined by the
10 group. They were kept at 18°C–24°C and relative humidity of 59%–61%, with a 12-h
11 light/dark cycle. Mice were fed a control common diet (CD) comprising 10% calories
12 from fat (D12450k) or an HFD comprising 60% calories from fat (D12492). They
13 then had ad libitum access to water (W or HGRW) and diet (CD or HFD), based on
14 group allocation. CD (D12450k) and HFD (D12492) were purchased from Shanghai
15 Biopike Biotechnology co. LTD (Shanghai, China).

16 After a 1-week acclimation period, the mice were randomly divided into four
17 groups of six mice by the type of diet and water: (1) CD-W; (2) CD-HGRW; (3)
18 HFD-W; and (4) HFD-HGRW. Mice were individually identified by ear punching.

19 ***Collection of general data, serum, liver, and feces samples***

20 Body weight was measured weekly at 09:00 h before the morning feeding using an
21 electronic balance. Fasting blood glucose was measured once a week after overnight
22 fasting (12 h), and detected by tail vein sampling with the blood glucose meter
23 (FreeStyle Optium Neo). For the oral glucose tolerance test (OGTT), mice were fasted
24 overnight (12 h), weighed, and given a glucose dose based on body weight (20%
25 glucose solution, 0.002 g/g body weight gavage) [17]. Glucose was tested from the
26 tails of mice before (0 min) and at 15, 30, 60, and 120 min after gavage. Mice feces
27 samples were collected once every 4 weeks, immediately frozen in liquid nitrogen,
28 and stored at –80°C. After 12 weeks, mice were anesthetized by intraperitoneal
29 injection with chloral hydrate 400mg/kg and meperidine 4mg/kg of animal body
30 weight. There is no signs of peritonitis were observed after the administration of

1 chloral hydrate and meperidine. At which point whole blood was collected from the
2 orbital venous plexus and allowed to clot by leaving it undisturbed at room
3 temperature. Serum samples were obtained by centrifuging at $1500 \times g$ for 10 min,
4 before being stored at -80°C . The mice were sacrificed by cervical dislocation, liver
5 tissues were immediately rinsed with cold phosphate-buffered saline, frozen in liquid
6 nitrogen, and kept at -80°C for analysis.

7 ***Biochemical assays***

8 Blood supernatants were obtained as serum after centrifugation at $1500 \times g$ for 10
9 minutes and stored at -80°C for analysis. Serum insulin levels were assessed using
10 ELISA assay kits (Elabscience, Wuhan, China). Serum concentrations of aspartate
11 aminotransferase (AST), alanine aminotransferase (ALT), high-density lipoprotein
12 cholesterol (HDL-C), low-density lipoprotein cholesterol (LDL-C), triglyceride (TG),
13 total cholesterol (T-Cho), and glucose were assessed by the 7020 chemical
14 autoanalyzer (Hitachi, Tokyo, Japan) according to the manufacturer's instructions.

15 ***Assessment of oxidative stress***

16 Liver tissue specimens were assayed for their superoxide dismutase (SOD) activity
17 and malondialdehyde (MDA) content according to the manufacturer's protocols,
18 before optical densities were measured in a microplate reader. Measurement of SOD
19 activity (U mL^{-1}) was at 550 nm for SOD, using the formula [(absorbance in control
20 group - absorbance in sample group)/absorbance in control group/50%].
21 Measurement of MDA content (nmol mL^{-1}) was at 450 nm, using the formula
22 [(absorbance of sample - absorbance of standard blank sample)/(absorbance of
23 standard sample - absorbance of standard blank solution) \times standard concentration
24 (10 nmol mL^{-1}). Finally, glutathione peroxidase (GSH-PX) activity was assessed by
25 a GSH-PX kit according to the manufacturer's protocols; sample absorbance was
26 determined at 412 nm on a microplate reader after the reaction.

27 ***Liver histology***

28 Liver was dissected and cut into small pieces, soaked in 4% paraformaldehyde for 24
29 h at room temperature, stored at 4°C for 24 h, dehydrated with ethanol, clarified with
30 xylene, and embedded in paraffin. Five-micron sections were cut and stained with

1 hematoxylin and eosin. Photographs of different sample areas were taken with an
2 Axiovert 40CFL microscope equipped with an AxioCamMRC digital camera (Zeiss,
3 Germany).

4 ***Microbiota analysis by 16S rRNA sequencing***

5 After the fecal samples were thawed, bacterial genomic DNA was extracted using a
6 QiAmp DNA Stool Mini Kit (Qiagen Ltd, UK) following the manufacturer's
7 procedures [18]. For the library construction, we used the two-step polymerase chain
8 reaction (PCR) to amplify the v3-v4 region of 16S rRNA. The specific primers used
9 in this experiment were 357F (5'-actcctagcggaggagag-3') and 806R
10 (5'-ggactachvgggtwtctaat-3'). The amplified target fragment was detected by 1.2%
11 agarose gel electrophoresis, and amplified products were used as templates for step
12 two of PCR amplification. The aim was to add the connectors, primers, and barcode
13 for the Illumina platform sequencing to both ends of the target segment. PCR products
14 were purified using Agencourt AMPure XP magnetic beads before being quantified by
15 FTC-3000TM real-time PCR [19]. The samples were mixed in the same molar ratio,
16 and the library was prepared and sequenced. The v3-v4 region of 16S rRNA was
17 sequenced by the NGS Illumina Miseq 2x300bp platform [20], and the original Fastq
18 data were obtained. Each sample was distinguished by a barcode, sequence quality
19 was controlled (Trimmomatic software) and filtered (FLASH software) [21-22], and
20 the sequence was spliced according to the overlap relationship. Finally, the optimized
21 sequence was obtained (Mothur, 1.39.5 software) and cluster analyzed with
22 UPARSE, using 97% similarity threshold to obtain representative sequences for
23 operational taxonomic units (OTUs). Based on the cluster analysis results for the
24 OTUs, we used R language to analyze diversity by the Simpson index, Shannon index,
25 ACE, Chao1, good coverage, and sequencing depth. The taxonomic information was
26 used to analyze the community structure statistically at each classification level. Beta
27 diversity among the samples was analyzed.

28 The above procedure was analyzed in the Python (2.7.13) R program [23]. LEfSE
29 analysis of effect size was used to analyze the community differences between groups,
30 and linear discriminant analysis was conducted according to the taxonomic

1 composition in different conditions (study groups), to identify the communities or
2 species that had significant differences in sample classification.

3 ***Statistical analysis***

4 Statistical analyses were performed using IBM SPSS Version 24 and graphics were
5 created in GraphPad Prism 7.0. All data are expressed as the means \pm standard
6 deviation (SD). Comparisons of statistical significance differences among groups
7 were performed by one-way or two-way analysis of variance, followed by
8 Student–Newman–Keuls multiple range test or the correction of p-values by Tukey’s
9 multiple comparisons test. Spearman relation analysis was used to assess the
10 correlation between the two variables. Logistic regression was used in the multivariate
11 analysis. In all cases, $P < 0.05$ was considered statistically significant.

12 **Results**

13 ***Effects of HGRW on physical and serum biochemical parameters***

14 Mice were fed experimental diets for 12 weeks. Those fed an HFD had higher
15 bodyweights than those fed a CD, and by the end of week 4, significant weight
16 differences were observed (Table 1). After week 12, HFD mice were 69% heavier
17 than CD mice ($P < 0.0001$). The use of HGRW had no effect on weight gain. Similar
18 results were obtained for fasting blood glucose (Table 2) and the OGTT glucose level
19 (Table 3). The OGTT results at 15, 30, 60, and 120 min indicated that blood glucose
20 was significantly higher in the HFD-W group than in the CD-W group (Table 3). At 30,
21 60, and 120 minutes, there were also significant differences in blood glucose between
22 the CD-HGRW and HFD-HGRW groups. At 30 and 60 min, blood glucose levels
23 were significantly higher in the HFD-HGRW than in the HFD-W groups.

24 The serum biochemical indicators in the mice are shown in fig. 1. Mice fed a
25 HFD had significantly higher serum TC, TG, and HDL-C levels ($P < 0.05$) (fig. 1C-E).
26 However, AST, ALT, TC, TG, LDL-L, HDL-L, and insulin levels were lower in the
27 HGRW group than in the W group, albeit without statistical significance ($P > 0.05$)
28 (fig.1A-G).

29 ***Effects of HGRW on oxidative stress indices***

1 The SOD, MDA, and GSH-PX content in liver homogenate is shown in fig. 1(H-J).
2 Neither HFD nor HGRW affected SOD in mice ($P > 0.05$) (fig. 1H). Although
3 GSH-PX activity in the HFD group was lower than in the CD group, the difference
4 was not statistically significant ($P > 0.05$) (fig. 1I). No appreciable difference in SOD,
5 GSH-PX activity, or MDA was seen with the use of HGRW. By contrast, the MDA
6 content was significantly increased in the HFD group compared with the CD group
7 among mice consuming W and HGRW ($P < 0.001$) (fig. 1J).

8 ***Effects of HGRW on liver histology***

9 Hematoxylin and eosin stained sections of liver tissue are shown in fig. 2. The liver
10 parenchyma of mice in the HFD group mostly showed steatosis (fig. 2C, 2D), with a
11 large number of enlarged cells scattered in the normal parenchyma. Hepatocyte
12 steatosis is characterized by enlarged hepatocytes with round vacuoles of varying
13 sizes in the cytoplasm. Although the liver had steatosis in both HFD groups, it was
14 more pronounced in the HFD-W group. The liver in the HFD-HGRW group showed
15 only mild, mainly microvascular, steatosis (fig. 2D). The liver parenchyma of mice in
16 the CD group showed no significant steatosis (fig. 2A and 2B).

17 ***HGRW modifies gut microbiota in HFD-fed mice***

18 To assess the changes in the intestinal microbial community of mice on a HFD caused
19 by HGRW, we used the Illumina MiSeq platform to sequence the variable region of
20 the 16S rRNA gene (v3–v4) in the feces of mice from each group. The results are
21 shown as OTUs using 97% as homologous cutoff values. The ACE, Chao1, and
22 Simpson indexes decreased, while the Shannon index increased, among the mice
23 treated with HFD. The opposite pattern was seen for mice treated with HGRW, but the
24 difference was not statistically significant ($P > 0.05$). The phylogenetic differences of
25 intestinal flora were evaluated by principal coordinates analysis based on the OTU
26 analysis (fig. 3A). The HFD group exhibited a microbiota that clustered distinctly
27 from that of the CD group, whereas the HGRW group only exhibited a microbiota that
28 was partially distinct from that of the W group. Hierarchical clustering also showed
29 that the microbial composition in the feces of the HFD group was significantly
30 different from that of the CD group (fig. 3B). The composition of microorganisms in

1 the HGRW group was slightly different from that in the W group. The analysis of
2 group similarities (ANOSIM) indicated that the differences between the HFD and CD
3 groups were significant using the weighted UniFrac method calculated using R values
4 of 0.65 ($P = 0.001$) (fig. 3C).

5 To assess the effects of HFD and HGRW on intestinal microbial composition, we
6 compared the relative abundance of the all taxa in each group (fig. 3). At phylum level,
7 the relative abundance of *Firmicutes* was significantly higher, while that of
8 *Bacteroidetes* was significantly lower, in the HFD group than in the CD group (fig.
9 3D). The relative abundance of *Firmicutes* in the HGRW group was slightly higher,
10 but without statistical significance. At the genus level, the microbiota of the HFD
11 group showed a significantly greater abundance of *Blautia*, *Parabacteroides*,
12 *Intestinimonas*, *Anaerotruncus*, and *Lactococcus* (fig. 3E), and a lower abundance of
13 *Lactobacillus*, compared with the CD group. In the HFD group, *Intestinimonas*,
14 *Anaerotruncus*, and *Oscillibacter* were significantly more abundant in the HGRW
15 subgroup than in the W subgroup. At the species level, *Parabacteroides goldsteinii*
16 was more abundant and *Lactobacillus murinus* was less abundant in the HFD group
17 than in the CD group. Also, the abundance of *Clostridiales bacterium CIEAF 020* was
18 higher in the HGRW group than in the W group. In the HFD group, those given
19 HGRW had more *Anaerotruncus sp. G3* and *Lachnospiraceae bacterium DW8*, but
20 less *Acinetobacter baumannii*, than the W group (fig. 3F).

21 Furthermore, the Spearman correlation matrix confirmed that the experimental
22 parameters and flora were related (fig. 4). LEfSe analysis of effect size revealed
23 significance ($LDA > 2$, $P < 0.05$) between the two group differences for nine genera
24 and five species (fig. 4A). There were significant correlations between all genera and
25 relevant laboratory indicators ($P < 0.05$). In the HFD-HGRW group, six genera were
26 negatively and four genera were positively correlated with these indicators. The
27 relative abundance of *Akkermansia muciniphila* in the HGRW group, a bacterium
28 involved in maintaining the metabolic balance of the body, was negatively correlated
29 with AST and LDL-L levels ($P < 0.05$) (fig. 4B). LEfSe analysis of effect size
30 revealed significance ($LDA > 2$, $P < 0.05$) between the HFD-HGRW and CD-HGRW

1 group differences for 24 genera and 26 species. In the HFD group, 17 genera were
2 positively correlated with body weight, OGTT glucose, ALT, AST, TG, TC, HDL-L,
3 LDL-L, GSH-PX, and MDA levels (fig. 4C). In addition, it was notable that
4 *Lactobacillus* was negatively correlated with body weight, OGTT glucose, ALT, TG,
5 TC, HDL-L, LDL-L, and MDA, but was positively correlated with GSH-PX.
6 *Anaerotruncus_sps3* and *Firmicutes bacterium ASF500* were negatively correlated
7 with GSH-PX. *Akkermansia* was negatively correlated with AST and LDL-L.
8 Laboratory index and intestinal flora analysis suggest that *Lactobacillus* is closely
9 related to MDA levels in tissues, although it is unclear if a decrease in *Lactobacillus*
10 will increase MDA levels.

11 **Discussion**

12 Hydrogen acts as a therapeutic and protective antioxidant against oxidative stress and
13 plays a protective role in the cells of almost all organs [24]. Oxidative stress can be
14 caused by a variety of factors, including strenuous exercise, inflammation, myocardial
15 infarction, blood stasis, and organ transplantation [25]. The complex and diverse
16 intestinal microbiome has a symbiotic relationship with the host, with important roles
17 in nutrient decomposition and transformation, immune invasion, and intestinal villus
18 development [26]. Diet can directly affect the composition and activity of colonizing
19 microorganisms. Therefore, we anticipated that interventions to HFDs could induce
20 changes in the composition and metabolism of the intestinal microbiota, with
21 hydrogen potentially mitigating or reversing the process. The results of this study
22 somewhat support this hypothesis.

23 Previous studies have shown that most intestinal flora metabolize hydrogen [27],
24 which suggests that HGRW could affect gut microbial composition. Our study found
25 that the richness and diversity of the intestinal microbiome in mice fed a HFD
26 increased significantly, with the relative abundance of 28 genera differing
27 significantly to that in the mice fed a CD. The relative abundance of nine genera was
28 significantly different between HGRW mice and W mice, with 16S rRNA gene
29 sequencing analysis showing a relatively higher relative abundance of *Ruminococcus*,

1 *Oscillibacter*, *Anaerotruncus*, *Intestinimonas*, *Akkermansia muciniphila*, and
2 *Clostridium sp. ID5* in the HGRW group. *Akkermansia muciniphila* has been shown
3 to be negatively associated with many diseases [28]. It can affect glucose metabolism,
4 lipid metabolism, and intestinal immunity as a potentially beneficial bacterium.
5 *Clostridium sp. ID5* can produce a variety of short-chain fatty acids (SCFAs) by using
6 glucose and glycerin fermentation to produce acetic acid, butyric acid, and propionic
7 acid [29]. In turn, these play an important role in maintaining normal function of the
8 intestinal barrier [30]. Studies have found that *Ruminococcus* can reduce the damage
9 of oxidative stress by decreasing reactive oxygen species levels and increasing SOD
10 and GSH-PX levels [31]. The results showed that the relative abundance of beneficial
11 bacteria in the intestinal flora of mice with HGRW increased significantly. Body
12 weight, OGTT glucose, and levels of TC, TG, HDL-L, and MDA increased
13 significantly after HFD but decreased non-significantly after HGRW intervention ($P >$
14 0.5). However, there were still some positive effects.

15 The relative abundances of each of the 12 taxa were significantly lower in the
16 HFD-HGRW group than in the HFD-W group. Among them, *Butyricicoccus*,
17 *Anaeroplasma*, and *Acinetobacter* were significantly reduced by the HGRW
18 intervention. *Acinetobacter* is a typical opportunistic pathogen [32], and given that a
19 HFD ordinarily leads to a relative increase in the abundance of pathogenic bacteria,
20 this reduction may be relevant. However, there were no substantial changes in the
21 indicators of liver function damage (AST and ALT) in mice after 12 weeks of HFD
22 intervention, and the pathological results indicated that fatty degeneration had already
23 existed in liver parenchymal cells. The results of hematoxylin and eosin staining of
24 the liver tissue indicated that steatosis was significantly less severe in the parenchyma
25 of mice in the HFD-HGRW group than in the HFD-only group. Although the
26 physiological characteristics of *Butyricicoccus*, *Anaeroplasma*, and *Acinetobacter*
27 need to be clarified, our data suggest that changes in their abundance can significantly
28 alter the degree of steatosis.

29 There were several limitations in this study. The number of mice used in this
30 study was limited. Increasing the sample size would provide more convincing results.

1 In this experiment, relevant indexes were measured after 12 weeks of feeding on a
2 HFD with hydrogen-rich water. It turns out that hydrogen-rich water would have been
3 beneficial to the body.

4 **Conclusions**

5 In summary, HGRW had a significant effect on the intestinal microbiome of mice,
6 affecting the structure and composition of microorganisms. Many studies have shown
7 that the antioxidant activity of hydrogen increases with increases in the hydrogen
8 concentration, with damage inhibition being dose-dependent [33].Therefore, we
9 speculate that hydrogen molecules, which may be administered by HGRW, play a
10 beneficial role in oxidative stress. Further studies should use fecal bacteria
11 transplantation to clarify the exact role of HGRW on the intestinal microbiome. In the
12 meantime, we conclude that oral HGRW has antioxidant and liver protective effects,
13 with the potential to improve the diversity, richness, and structure of intestinal flora,
14 as well as enhancing the relative abundance of beneficial flora.

15 **Acknowledgments**

16 This study was supported by Hangzhou Yishui Technology co. LTD. We acknowledge
17 the hydrogen production equipment assistance provided by the company.

18 **Authors' contributions**

19 JXX participated in the study conception and design. All authors contributed to
20 material preparation, data collection and analysis. The manuscript was written by GJX
21 and ZLL. All authors read and approved the final manuscript.

22 **Funding**

23 This research was funded by National Natural Science Funds of China (No. 81760168)
24 and Jiangxi Provincial Natural Science Funds of China (No. 20192BAB205031).

25 **Availability of data and materials**

26 The datasets used and/or analyzed during the current study are available from the

1 corresponding author on reasonable request.

2 **Ethics approval and consent to participate**

3 The protocol of animal experiments was approved by Medical Research Ethics
4 Committee of The First Affiliated Hospital of Nanchang University, Nanchang, China.
5 The animal experiment conforms to the ethics requirements, ethics number is (2018)
6 medical research no.(064).

7 **Consent for publication**

8 Not applicable.

9 **Competed interests**

10 The authors do not have any competed interests.

11 **Publisher's Note**

12 Springer Nature remains neutral with regard to jurisdictional claims in published
13 maps and institutional affiliations.

14 **References**

- 15 1. Nishida AH, Ochman H. A great-ape view of the gut microbiome. *NAT REV*
16 *GENET.* 2019; 20: 195-206.
- 17 2. Sommer F, Anderson JM, Bharti R, Raes J, Rosenstiel P. The resilience of the
18 intestinal microbiota influences health and disease. *NAT REV MICROBIOL.* 2017;
19 15: 630-38.
- 20 3. Gentile CL, Weir TL. The gut microbiota at the intersection of diet and human
21 health. *SCIENCE.* 2018; 362: 776-80.
- 22 4. Brial F, Le Lay A, Dumas ME, Gauguier D. Implication of gut microbiota
23 metabolites in cardiovascular and metabolic diseases. *CELL MOL LIFE SCI.*
24 2018; 75: 3977-90.
- 25 5. Sommer F, Backhed F. The gut microbiota--masters of host development and
26 physiology. *NAT REV MICROBIOL.* 2013; 11: 227-38.

- 1 6. Macpherson AJ, Harris NL. Interactions between commensal intestinal bacteria
2 and the immune system. *NAT REV IMMUNOL*. 2004; 4: 478-85.
- 3 7. Vaarala O, Atkinson MA, Neu J. The "perfect storm" for type 1 diabetes: the
4 complex interplay between intestinal microbiota, gut permeability, and mucosal
5 immunity. *DIABETES*. 2008; 57: 2555-62.
- 6 8. Sanna S, van Zuydam NR, Mahajan A, Kurilshikov A, Vich VA, Vosa U, *et al.*
7 Causal relationships among the gut microbiome, short-chain fatty acids and
8 metabolic diseases. *NAT GENET*. 2019; 51: 600-05.
- 9 9. Boulange CL, Neves AL, Chilloux J, Nicholson JK, Dumas ME. Impact of the
10 gut microbiota on inflammation, obesity, and metabolic disease. *GENOME MED*.
11 2016; 8: 42.
- 12 10. Fruhbeck G, Gomez-Ambrosi J, Rodriguez A, Ramirez B, Valenti V, Moncada R,
13 *et al.* Novel protective role of kallistatin in obesity by limiting adipose tissue low
14 grade inflammation and oxidative stress. *METABOLISM*. 2018; 87: 123-35.
- 15 11. Manna P, Jain SK. Obesity, Oxidative Stress, Adipose Tissue Dysfunction, and
16 the Associated Health Risks: Causes and Therapeutic Strategies. *Metab Syndr*
17 *Relat Disord*. 2015; 13: 423-44.
- 18 12. Kehrer JP, Klotz LO. Free radicals and related reactive species as mediators of
19 tissue injury and disease: implications for Health. *CRIT REV TOXICOL*. 2015; 45:
20 765-98.
- 21 13. Poprac P, Jomova K, Simunkova M, Kollar V, Rhodes CJ, Valko M. Targeting
22 Free Radicals in Oxidative Stress-Related Human Diseases. *TRENDS*
23 *PHARMACOL SCI*. 2017; 38: 592-607.
- 24 14. Cejka C, Kubinova S, Cejkova J. The preventive and therapeutic effects of
25 molecular hydrogen in ocular diseases and injuries where oxidative stress is
26 involved. *Free Radic Res*. 2019; 53: 237-47.
- 27 15. Affane F, Louala S, El IHN, Bensalah F, Chekkal H, Allaoui A, *et al.*
28 Hypolipidemic, antioxidant and antiatherogenic property of sardine by-products
29 proteins in high-fat diet induced obese rats. *LIFE SCI*. 2018; 199: 16-22.
- 30 16. Higashimura Y, Baba Y, Inoue R, Takagi T, Uchiyama K, Mizushima K, *et al.*

- 1 Effects of molecular hydrogen-dissolved alkaline electrolyzed water on intestinal
2 environment in mice. *Med Gas Res.* 2018; 8: 6-11.
- 3 17. Steenberg VR, Jensen SM, Pedersen J, Madsen AN, Windelov JA, Holst B, *et al.*
4 Acute disruption of glucagon secretion or action does not improve glucose
5 tolerance in an insulin-deficient mouse model of diabetes. *DIABETOLOGIA.*
6 2016; 59: 363-70.
- 7 18. Qi C, Li Y, Yu RQ, Zhou SL, Wang XG, Le GW, *et al.*. Composition and
8 immuno-stimulatory properties of extracellular DNA from mouse gut flora. *World*
9 *J Gastroenterol.* 2017; 23: 7830-39.
- 10 19. Malinen E, Rinttila T, Kajander K, Matto J, Kassinen A, Krogius L, *et al.*
11 Analysis of the fecal microbiota of irritable bowel syndrome patients and healthy
12 controls with real-time PCR. *AM J GASTROENTEROL.* 2005; 100: 373-82.
- 13 20. Fadrosch DW, Ma B, Gajer P, Sengamalay N, Ott S, Brotman RM, *et al.*. An
14 improved dual-indexing approach for multiplexed 16S rRNA gene sequencing on
15 the Illumina MiSeq platform. *MICROBIOME.* 2014; 2: 6.
- 16 21. Bolger AM, Lohse M, Usadel B. Trimmomatic: a flexible trimmer for Illumina
17 sequence data. *BIOINFORMATICS.* 2014; 30: 2114-20.
- 18 22. Matsushima A, Kobayashi N, Mochizuki Y, Ishii M, Kawaguchi S, Endo TA, *et*
19 *al.*. OmicBrowse: a Flash-based high-performance graphics interface for genomic
20 resources. *NUCLEIC ACIDS RES.* 2009; 37: W57-62.
- 21 23. Misner I, Bicep C, Lopez P, Halary S, Baptiste E, Lane CE. Sequence
22 comparative analysis using networks: software for evaluating de novo transcript
23 assembly from next-generation sequencing. *MOL BIOL EVOL.* 2013; 30:
24 1975-86.
- 25 24. Ohsawa I, Ishikawa M, Takahashi K, Watanabe M, Nishimaki K, Yamagata K, *et*
26 *al.*. Hydrogen acts as a therapeutic antioxidant by selectively reducing cytotoxic
27 oxygen radicals. *NAT MED.* 2007; 13: 688-94.
- 28 25. Lechuga-Sancho AM, Gallego-Andujar D, Ruiz-Ocana P, Visiedo FM,
29 Saez-Benito A, Schwarz M, *et al.*. Obesity induced alterations in redox
30 homeostasis and oxidative stress are present from an early age. *PLOS ONE.* 2018;

- 1 13: e191547.
- 2 26. Fung TC, Olson CA, Hsiao EY. Interactions between the microbiota, immune and
3 nervous systems in health and disease. *NAT NEUROSCI*. 2017; 20: 145-55.
- 4 27. Hylemon PB, Harris SC, Ridlon JM. Metabolism of hydrogen gases and bile
5 acids in the gut microbiome. *FEBS LETT*. 2018; 592: 2070-82.
- 6 28. Naito Y, Uchiyama K, Takagi T. A next-generation beneficial microbe:
7 *Akkermansia muciniphila*. *J CLIN BIOCHEM NUTR*. 2018; 63: 33-35.
- 8 29. Ramachandran U, Wrana N, Cicek N, Sparling R, Levin DB. Isolation and
9 characterization of a hydrogen- and ethanol-producing *Clostridium* sp. strain
10 URNW. *CAN J MICROBIOL*. 2011; 57: 236-43.
- 11 30. LeBlanc JG, Chain F, Martin R, Bermudez-Humaran LG, Courau S, Langella P.
12 Beneficial effects on host energy metabolism of short-chain fatty acids and
13 vitamins produced by commensal and probiotic bacteria. *MICROB CELL FACT*.
14 2017; 16: 79.
- 15 31. Park J, Lee J, Yeom Z, Heo D, Lim YH. Neuroprotective effect of *Ruminococcus*
16 *albus* on oxidatively stressed SH-SY5Y cells and animals. *Sci Rep*. 2017; 7:
17 14520.
- 18 32. Asahara T, Takahashi A, Yuki N, Kaji R, Takahashi T, Nomoto K. Protective
19 Effect of a Synbiotic against Multidrug-Resistant *Acinetobacter baumannii* in a
20 Murine Infection Model. *Antimicrob Agents Chemother*. 2016; 60: 3041-50.
- 21 **33.** Xue J, Shang G, Tanaka Y, Saihara Y, Hou L, Velasquez N, *et al.*. Dose-dependent
22 inhibition of gastric injury by hydrogen in alkaline electrolyzed drinking water.
23 *BMC Complement Altern Med*. 2014; 14: 81.

1 **Table 1** Effects of HGRW treatment on the animal model's body weight(g)

Time	CD-W	CD-HGRW	HFD-W	HFD-HGRW
0 wk	22.2±1.03	21.6±1.36	22.3±0.88	22.2±1.13
2 wk	23.6±1.16	23.1±1.16	25.7±0.60	26.0±2.14 ##
4 wk	23.8±1.23	22.8±1.24	26.7±0.54 *	27.5±2.65 #####
6 wk	25.3±1.35	24.7±1.09	28.8±0.88 **	29.9±3.00 #####
8 wk	24.8±1.53	23.6±1.37	29.6±0.87 *****	30.7±3.81 #####
10 wk	25.4±1.39	24.6±1.50	31.6±1.21 *****	32.6±4.18 #####
12 wk	23.9±1.44	23.1±1.23	30.3±0.86 *****	31.2±4.03 #####

2 Note: Values are expressed as mean± SD ,and analyzed by Tukey's multiple
 3 comparisons test . *p<0.05 versus the CD-W group. **p<0.01 versus the CD-W
 4 group. ***p<0.0001 versus the CD-W group.## p<0.01 versus the CD-HGRW
 5 group.##### p<0.0001 versus the CD-HGRW group.

6 **Table 2** Effects of HGRW treatment on the animal model's fasting blood
 7 glucose(mmol/L)

Time	CD-W	CD-HGRW	HFD-W	HFD-HGRW
0 wk	4.5±0.53	4.2±0.47	4.8±0.51	4.4±0.59
4 wk	4.2±0.73	4.0±0.59	5.4±0.98 *	4.9±0.96
8 wk	4.9±0.48	5.0±0.70	5.9±0.76	4.9±0.73
12 wk	5.8±0.63	6.2±0.70	6.1±0.59	5.5±1.00

8 Note: Values are expressed as mean± SD ,and analyzed by Tukey's multiple
 9 comparisons test .

10 *p<0.05 versus the CD-W group.

11 **Table 3** Effects of HGRW treatment on the animal model's oral glucose tolerance
 12 test (OGTT) glucose level (mmol/L)

Time	CD-W	CD-HGRW	HFD-W	HFD-HGRW
0min	5.8±0.63	6.2±0.70	6.1±0.59	5.5±1.00
15min	11.8±1.46	17.2±3.48	18.1±1.68 ****	19.1±2.78
30min	9.3±1.36	10.5±1.15	14.6±2.08 ****	20.2±2.74 #####++++
60min	8.1±1.45	8.5±0.93	12.2±1.11 ***	15.3±2.87 ##### +
120min	6.8±0.96	7.1±0.55	10.3±1.04 **	10.7±1.51 ##

1 Note: Values are expressed as mean± SD ,and analyzed by Tukey’s multiple
2 comparisons test . *p<0.05 versus the CD-W group. **p<0.01 versus the CD-W
3 group. ***p<0.001 versus the CD-W group. ****p<0.0001 versus the CD-W
4 group. ## p<0.01 versus the CD-HGRW group. ##### p<0.0001 versus the
5 CD-HGRW group. +p<0.05 versus the HFD-W group. ++++p<0.0001 versus
6 the HFD-W group.

7 **fig. legends**

8 **fig. 1.** Effects of HGRW on serum and tissue biochemical parameters and oxidative
9 stress indices. A-B: Serum transaminase levels were tested. C-F: Serum lipid levels
10 were tested. G: Insulin levels were tested. H-I: Hepatic activities of antioxidant
11 enzyme levels were tested; J: Hepatic levels of MDA were shown as markers of
12 oxidative stress. The values are the mean ± SD from six mice. NS means P > 0.05, *
13 means P < 0.05, ** means P < 0.01, and *** means P < 0.001.

14 **fig. 2.** Histological sections stained by hematoxylin and eosin of livers from group
15 CD-W (A), CD-HGRW (B), HFD-W (C), and HFD-HGRW (D). Prominent hepatic
16 steatosis was observed in mice fed a HFD. Arrow in picture (C) indicates
17 macrovesicular inclusions, whereas arrow in picture (D) indicates microvesicular
18 inclusions.

1 **fig. 3.** Modulation of HGRW on the structure and composition of gut microbiota in
2 mice.

3 Principal coordinate analysis (PCoA) (A) and sample clustering results (B) at the
4 phylum level of the weighted UniFrac distances of microbial 16S rRNA sequences
5 from the V3-V4 regions in the stool samples. ANOSIM analysis indicated that the
6 differences between the groups were significant ($R = 0.65$, $P < 0.001$) (C). Phylum
7 level (D), genus level (E) and species level (F) taxonomic distributions of the
8 microbial communities in the stool samples ascertained from next-generation
9 sequencing. The right graph portrays significantly different taxa in different groups.
10 Data represent the means \pm SE of six mice.*means $P < 0.05$, **means $P < 0.01$,
11 ***means $P < 0.001$, ****means $P < 0.0001$ (ANOVA test).

12 **fig. 4.** Spearman correlation analysis of clinical data and the intestinal microbiota
13 based on LEfSe analysis results. LEfSe identified the taxa with the greatest
14 differences in abundance between the HFD-HGRW and HFD-W groups. At the genus
15 and species levels, the HFD-W group-enriched taxa are indicated by a positive LDA
16 score (green) and HFD-HGRW group-enriched taxa are indicated by a negative score
17 (red). Only taxa meeting a significant LDA threshold value of >2 are shown (A).
18 Heatmaps showing correlations between clinical factors and gut microbiota at genus
19 and species levels were estimated using Spearman correlation analysis. HFD-HGRW
20 and HFD-W groups are shown in (B). HFD-HGRW and CD-HGRW groups are
21 shown in (C). Color intensity represents the magnitude of correlation. Red means
22 positive correlations; blue means negative correlations. * denotes adjusted $P < 0.05$;
23 ** denotes adjusted $P < 0.01$.

Figures

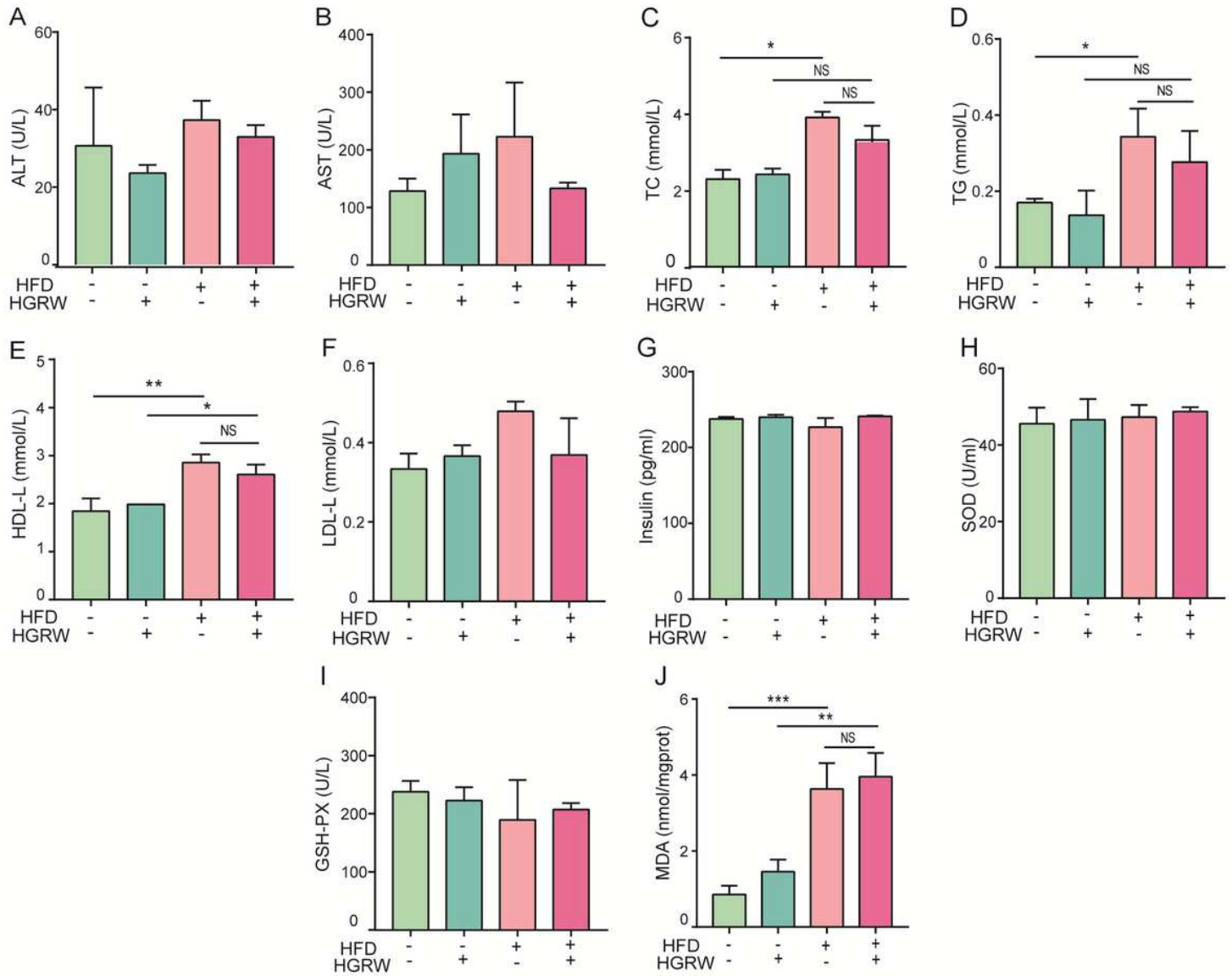


Figure 1

Effects of HGRW on serum and tissue biochemical parameters and oxidative stress indices. A-B: Serum transaminase levels were tested. C-F: Serum lipid levels were tested. G: Insulin levels were tested. H-I: Hepatic activities of antioxidant enzyme levels were tested; J: Hepatic levels of MDA were shown as markers of oxidative stress. The values are the mean \pm SD from six mice. NS means $P > 0.05$, * means $P < 0.05$, ** means $P < 0.01$, and *** means $P < 0.001$.

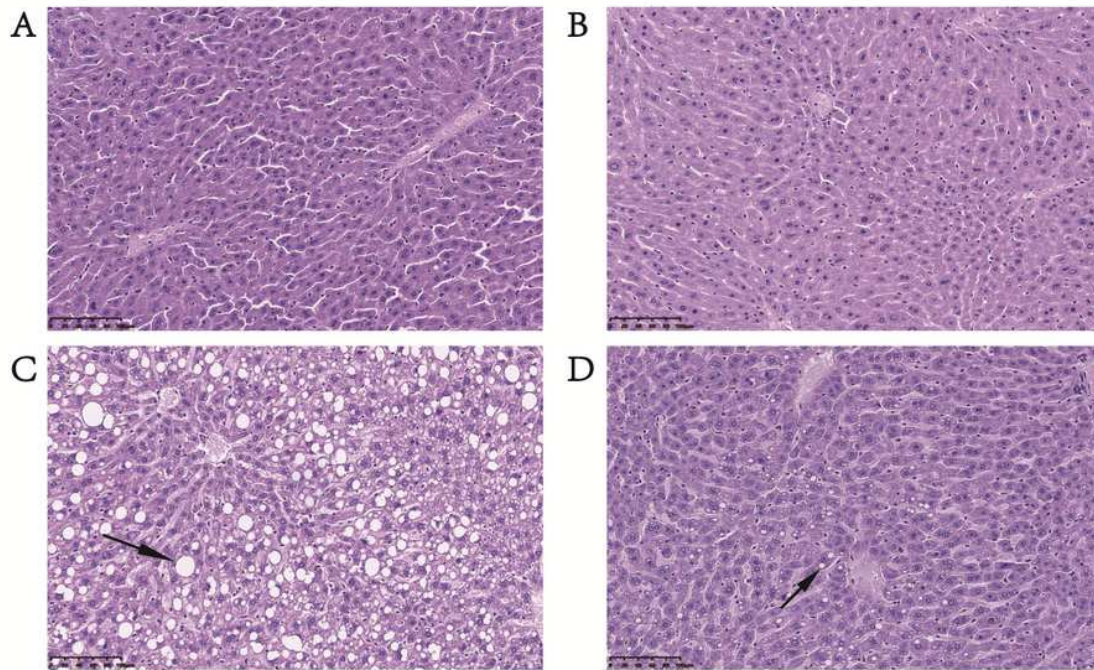


Figure 2

Histological sections stained by hematoxylin and eosin of livers from group CD-W (A), CD-HGRW (B), HFD-W (C), and HFD-HGRW (D). Prominent hepatic steatosis was observed in mice fed a HFD. Arrow in picture (C) indicates macrovesicular inclusions, whereas arrow in picture (D) indicates microvesicular inclusions.

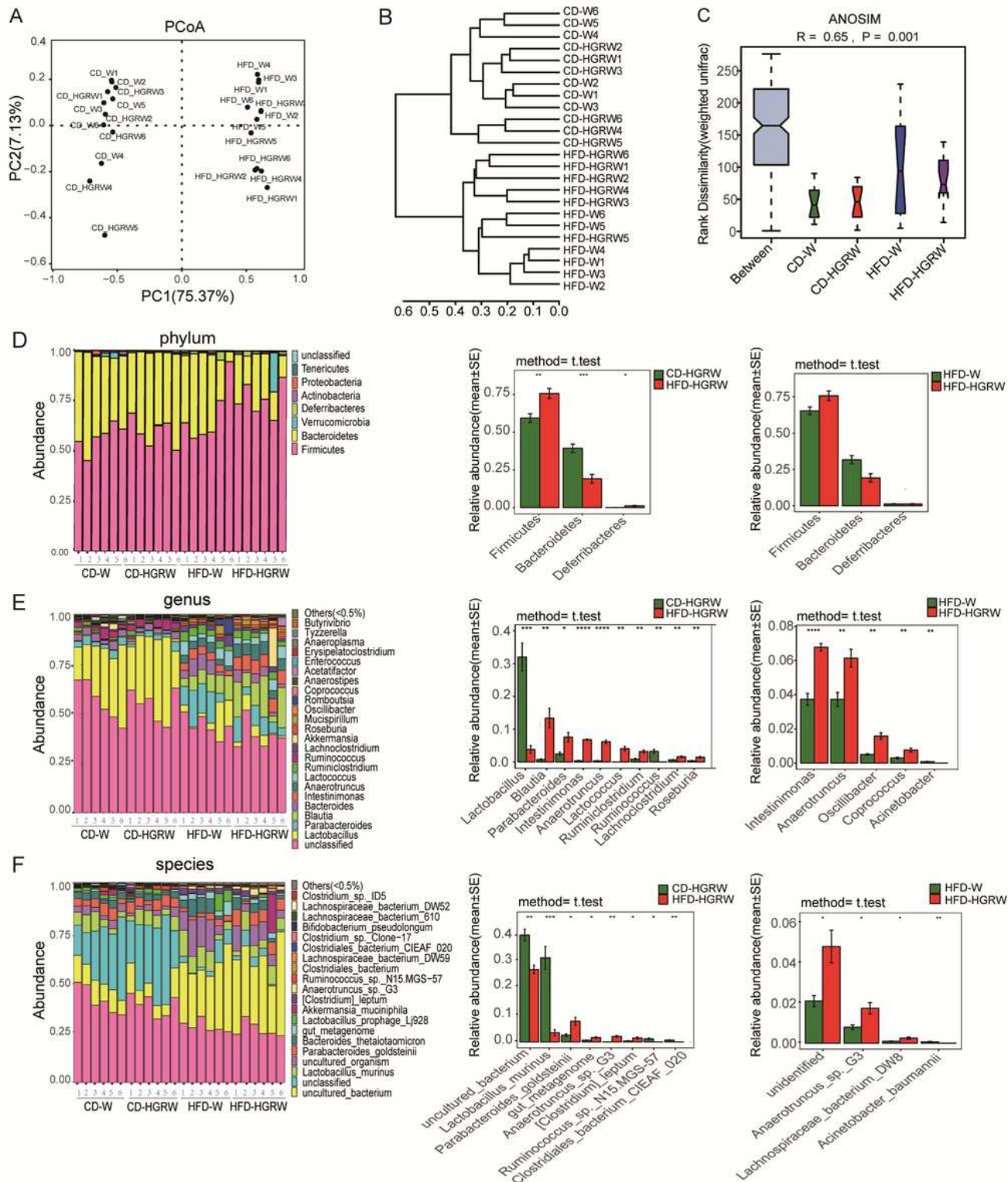


Figure 3

Modulation of HGRW on the structure and composition of gut microbiota in mice. Principal coordinate analysis (PCoA) (A) and sample clustering results (B) at the phylum level of the weighted UniFrac distances of microbial 16S rRNA sequences from the V3-V4 regions in the stool samples. ANOSIM analysis indicates that the differences between the groups were significant ($R = 0.65$, $P < 0.001$) (C). Phylum level (D), genus level (E) and species level (F) taxonomic distributions of the microbial

communities in the stool samples ascertained from next-generation sequencing. The right graph portrays significantly different taxa in different groups. Data represent the means \pm SE of six mice. *means $P < 0.05$, **means $P < 0.01$, ***means $P < 0.001$, ****means $P < 0.0001$ (ANOVA test).

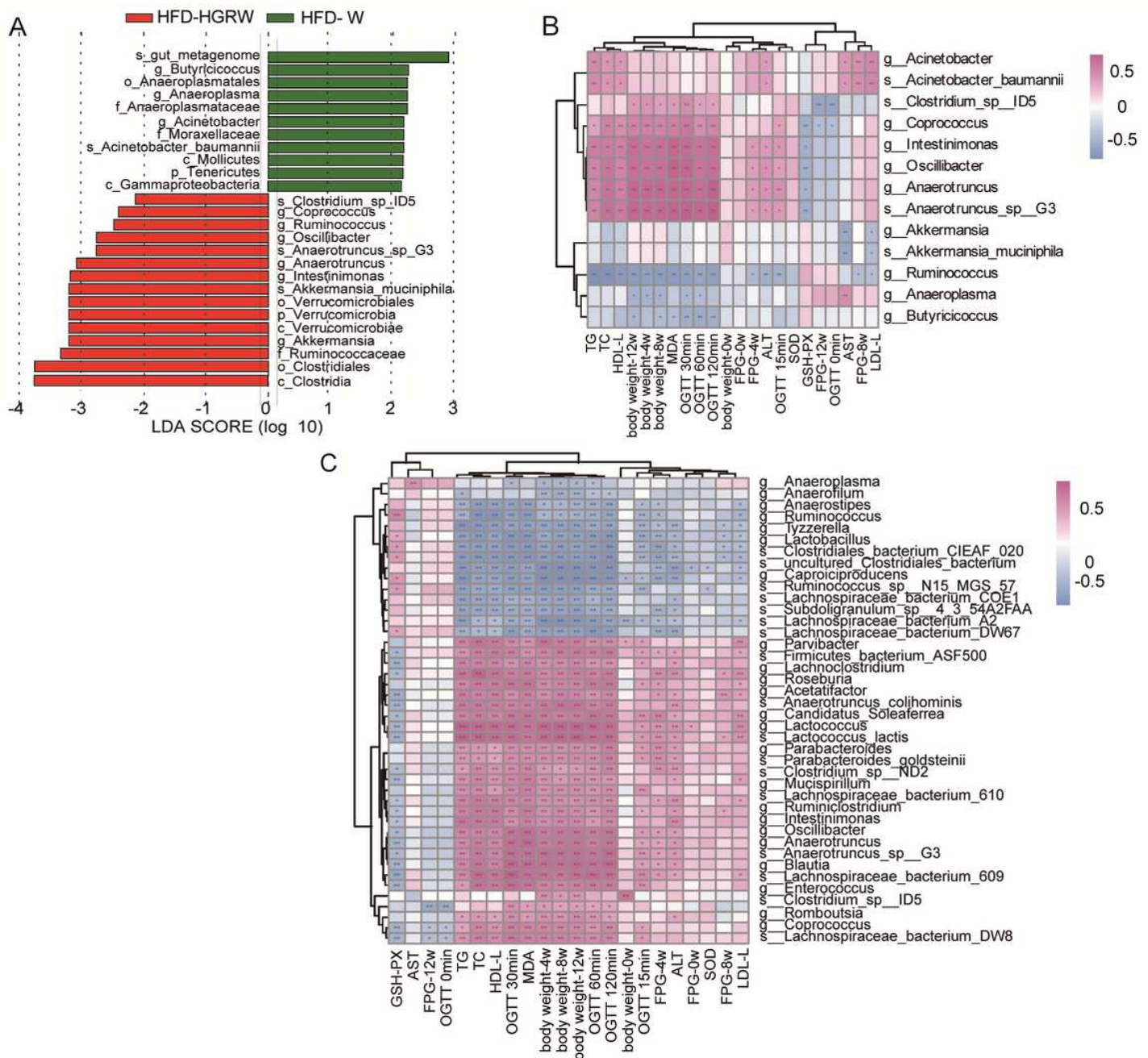


Figure 4

Spearman correlation analysis of clinical data and the intestinal microbiota based on LefSe analysis results. LefSe identified the taxa with the greatest differences in abundance between the HFD-HGRW and HFD-W groups. At the genus and species levels, the HFD-W group-enriched taxa are indicated by a positive LDA score (green) and HFD-HGRW group-enriched taxa are indicated by a negative score (red). Only taxa meeting a significant LDA threshold value of >2 are shown (A). Heatmaps showing correlations between clinical factors and gut microbiota at genus and species levels were estimated using Spearman correlation analysis. HFD-HGRW and HFD-W groups are shown in (B). HFD-HGRW and CD-HGRW groups

are shown in (C). Color intensity represents the magnitude of correlation. Red means positive correlations; blue means negative correlations. * denotes adjusted $P < 0.05$; ** denotes adjusted $P < 0.01$.